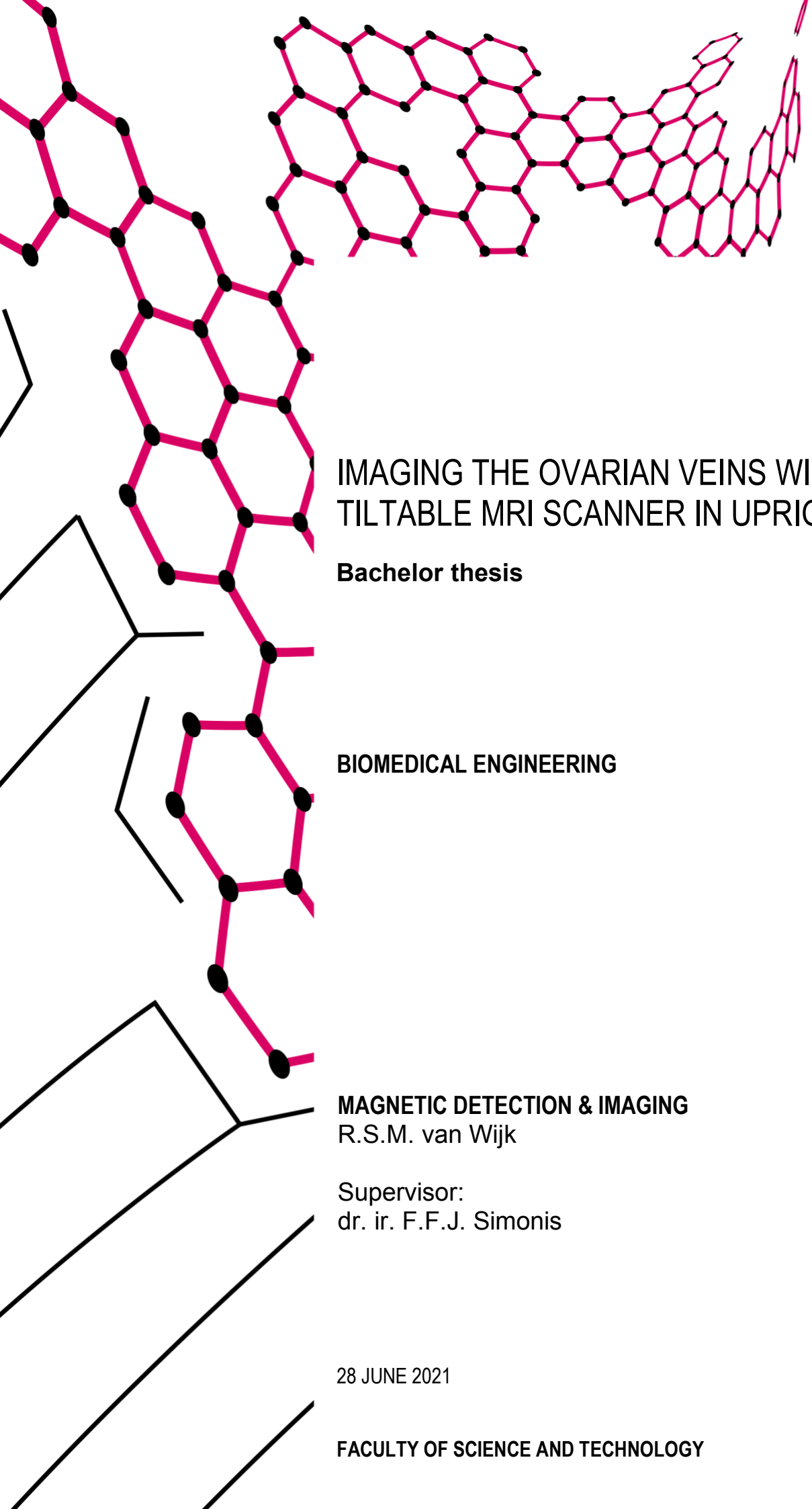

IMAGING THE OVARIAN VEINS WITH A 0,25 T TILTABLE MRI SCANNER IN UPRIGHT POSITION

Bachelor thesis

BIOMEDICAL ENGINEERING

MAGNETIC DETECTION & IMAGING
R.S.M. van Wijk

Supervisor:
dr. ir. F.F.J. Simonis

28 JUNE 2021

FACULTY OF SCIENCE AND TECHNOLOGY UNIVERSITY OF TWENTE

ABSTRACT

Het doel van dit onderzoek is om de vena ovarica in beeld te brengen bij gezonde vrouwelijke proefpersonen met behulp van de $0,25$ T kantelbare MRI-scanner in staande positie, en daarmee een optimaal beeldvormingsprotocol te ontwikkelen voor het afbeelden van de vena ovarica in staande positie. Het uitvoeren van MRI in staande positie kan namelijk mogelijk bijdragen aan het diagnosticeren van *Pelvic Venous Congestion Syndrome*, afgekort PVCS. Door MRI uit te voeren in staande positie zullen de vena ovarica verwijden, waardoor de bekken varices, als gevolg van PVCS, mogelijk duidelijker zichtbaar zijn in de verkregen afbeeldingen. Wanneer met zekerheid kan worden gesteld dat de beide vena ovarica in beeld gebracht kunnen worden bij gezonde vrouwelijke proefpersonen, kan verder onderzoek worden gedaan naar hoe deze techniek mogelijk kan bijdragen aan het diagnosticeren van PVCS.

Om een optimaal beeldvormingsprotocol te ontwikkelen voor het afbeelden van de vena ovarica met de $0,25$ T kantelbare MRI-scanner in staande positie, is allereerst geprobeerd de vena ovarica in beeld te brengen met behulp van een $1,5$ T MRI-scanner in liggende positie. Op deze manier kan worden bepaald of de vena ovarica met een hogere veldsterkte in beeld gebracht kunnen worden, en kan achterhaald worden wat de exacte locatie is.
De volgende afbeeldingssequenties zijn uitgevoerd op $1,5$ T in liggende positie: T_2-gewogen fast spin echo sequentie, een time-of-flight sequentie, een T_1-gewogen Dixon sequentie en een phase contrast MRA sequentie. De sequenties die een contrast verkregen waarbij de vena ovarica zichtbaar zijn op $1,5$ T in liggende positie, zijn opnieuw uitgevoerd bij $0,25$ T in staande positie. Op $0,25$ T in staande positie is opnieuw gekeken of de overgebleven sequenties een contrast verkregen waarbij de vena ovarica zichtbaar zijn. Waarna vervolgens een optimaal beeldvormingsprotocol kan worden ontwikkeld voor het in beeld brengen van de vena ovarica in staande positie.

Enkel met behulp van de T_2-gewogen fast spin echo sequentie is een contrast verkregen waarbij de linker vena ovarica is afgebeeld op $1,5$ T in liggende positie. Bij de andere uitgevoerde sequenties was het contrast niet juist voor het identificeren van de linker vena ovarica en/of rechter vena ovarica. Om deze reden is enkel de T_2-gewogen fast spin echo sequentie uitgevoerd bij de $0,25$ T kantelbare MRI-scanner in staande positie. Bij een veldsterkte van $0,25$ T in staande positie werden ook structuren afgebeeld die mogelijk de linker vena ovarica zouden kunnen zijn. Echter, door artefacten als gevolg van darmperistaltiek en het niet kunnen volgen van het verloop van deze structuren, was het lastig om dit met zekerheid vast te kunnen stellen. De rechter vena ovarica kon niet in beeld gebracht worden.

Het afbeelden van de beide vena ovarica met behulp van de $0,25$ T kantelbare MRI-scanner in staande positie is gedurende dit onderzoek nog niet succesvol geweest. Desondanks, kan er geconcludeerd worden dat het beeldvormingsprotocol voor het afbeelden van de vena ovarica in staande positie wel de T_2-gewogen fast spin echo sequentie uitgevoerd in axiaal vlak moet omvatten. Met behulp van deze sequentie kan namelijk een contrast worden verkregen, waarmee de vena ovarica kunnen worden geïdentificeerd. Er zal verder onderzoek moeten worden gedaan om dit beeldvormingsprotocol te optimaliseren, zodat beide vena ovarica afgebeeld en geïdentificeerd kunnen worden in staande positie met behulp van de $0,25$ T kantelbare MRI-scanner.

TABLE OF CONTENTS

1 INTRODUCTION

Chronic pelvic pain is a common condition among women. The prevalence of chronic pelvic pain among the global female population is estimated between 2.1 to 24%. Chronic pelvic pain is defined as a pain in the abdomen or pelvis that lasts for at least six months. The causes of chronic pelvic pain are varied [1].

A common cause of chronic pelvic pain is *Pelvic Venous Congestion Syndrome* (PVCS). This condition causes 16 to 31% of the cases of chronic pelvic pain [2]. PVCS arises from a reflux of blood in the ovarian veins and/or iliac veins. This reflux can lead to pelvic varices.
It is thought that the reflux of blood in the ovarian veins and/or iliac veins could have three different causes, but the exact etiology remains uncertain. First, the reflux can be caused by valvular insufficiency. This involves the absence or deficient functioning of the venous valves, which can cause the blood in the ovarian veins to flow back i.e., reflux of the blood. Another possible cause is venous obstruction. This can arise because of extrinsic compression. This extrinsic compression can be caused by various syndromes, for example the Nutcracker syndrome and the May-Thurner syndrome [3]. The left ovarian vein is often the most affected by venous compression due to the anatomical position [4]. In addition to valvular insufficiency and venous obstruction, hormones can also play an important role in the development of the reflux, especially in the ovarian veins. The ovarian veins are sensitive to estrogen-mediated vasodilation. During the menstrual cycle, the ovarian veins are exposed to very high levels of estrogen, which can lead to dilation. This dilation can again lead to valvular insufficiency, venous reflux and eventually pelvic varices. However, a lot of research is still being done on the hormonal cause of PVCS [2].
Research shows that most cases of pelvic varices are found in the ovarian veins. PVCS has been developed in 60% of these cases [3].

Contrast venography is considered to be the diagnostic standard for assessing pelvic varices, and hence for diagnosing PVCS. However, this uses contrast material and ionizing, which is damaging for the patient. Therefore, ultrasound is also widely used in patients with suspected PVCS. Nevertheless, ultrasound is limited by a high false-positive rate, low image quality and small field of view [3]. For these reasons, MRI is suggested. MRI provides a detailed anatomic overview and no ionizing is required. However, MRI is often performed in supine position, where the ovarian veins will be less dilated, and the varices will be less visible in the images. The use of a MRI scanner in upright position can be a solution for this. Previous research has already been done on imaging the ovarian veins in semi-upright position by using ultrasound for diagnosing PVCS. This research showed that the diameter of the ovarian veins were already more increased while imaging in semi-upright position [5]. Therefore by using a MRI scanner in upright position, the ovarian veins may be more dilated, and the varices can become clearly visible in the images. Which may contribute to diagnosing PVCS.

Based on these findings, the goal of this thesis will be to image the ovarian veins in healthy female volunteers with the help of a MRI scanner in upright position, and with that determine which imaging sequences can be used for imaging the ovarian veins in upright position. This leads to the following research question that will be answered in this thesis:

- *What can be an optimal imaging protocol for imaging the ovarian veins with a $0,25$ T MRI scanner in upright position?*

When it can be stated with certainty that the ovarian veins can be imaged in upright position in healthy female volunteers, further research can be done on how this technique can contribute to diagnose PVCS.

2 METHOD

2.1 MRI

To develop an optimal imaging protocol for imaging the ovarian veins with a $0,25$ T MRI scanner in upright position, the ovarian veins will first be tried to be imaged with a $1,5$ T MRI scanner in supine position. In this way it can be determined whether the ovarian veins can be imaged with a higher field strength of $1,5$ T, and if this is the case what their location is. Because a field strength of $0,25$ T is relatively low, locating the ovarian veins first in images acquired at $1,5$ T in supine position could help locate the ovarian veins in images acquired at $0,25$ T in upright position.

Various imaging sequences will first be performed at $1,5$ T in supine position. The sequences that will be performed will be explained and substantiated in section 2.3. The sequences that obtain a contrast at which the ovarian veins may not be visible at $1,5$ T in supine position, will be eliminated. The sequences that obtain a contrast at which the ovarian veins are visible will be performed at $0,25$ T in upright position. Likewise, at $0,25$ T it will be determined which of the remaining imaging sequences can image the ovarian veins. After which an imaging protocol can be developed for imaging the ovarain veins in upright position.

All images that will be made will be acquired on two MRI scanners that are available at the TechMed Center of the University of Twente:

- The $1,5$ T clinical scanner (Magnetom Aera, Siemens Healthineers, Germany), which allows the acquisition of high-quality non-contrast MRI in supine position.
- The specialized $0,25$ T tiltable scanner (G-scan Brio, Esaote SpA, Italy), which allows the acquisition of scans in both supine and upright position.

For scanning with the two MRI scanners healthy female volunteers will be asked. These volunteers will be screened based on a screening list. In this way, the volunteers will enter the MRI safely.

The scans will be acquired with the *Ultraflex Large 18 coil* in the $1,5$ T clinical scanner and with the *4 Channel Lumbar Spine coil* in the $0,25$ T tiltable scanner. The images will be acquired of the abdomen and pelvis, without the use of contrast agents. This is because the scans will be made of healthy volunteers, and there is a possible link between gadolinium-based contrast agents and nephrogenic systemic fibrosis [6].

2.2 Assessment of the images

A sequence will be considered useful if the obtained contrast can visualise the ovarian veins in the images. If this is not the case, the sequence will be eliminated, this as previously stated. As mentioned before, a dilated diameter of the ovarian veins may indicate PVCS [2]. Therefore, it is important that in the images that will be acquired the diameter of the ovarian veins will be visible.

When assessing the images, it is important to take the anatomy into consideration. By following different anatomical structures, the course of the ovarian veins can be visualised, and with that the ovarian veins can be identified in the images. In figure 2.1 the white arrow points to the right ovarian vein (ROV), and the yellow arrow points to the left ovarian vein (LOV).

As shown in the figure, both the LOV and ROV arise respectively from the left and right ovary. Closely to the ovarian arteries and the ureter, the ovarian veins run up into the pelvis and abdomen. This as shown in the figure. The LOV then drains into the left renal vein (LRV). Contrary to the ROV, which drains directly into the inferior vena cava (IVC). This is an important difference in anatomical course for the LOV and ROV, and can be used as a starting point for identifying the ovarian veins in the images. Both the left ovarian artery (LOA) and right ovarian artery (ROA) branches from the aorta [7].

Thus, if the ovarian veins are to be identified in a series of images, it is important to find the drainage of the ovarian veins. Whereas the LOV is drained into the LRV and the ROV directly into the IVC. When the drainage of both the ovarian veins is found in the series of images, the course can be followed, and if it concerns the ovarian veins, it will lead to the ovaries.

The images will also be assessed by a lab technician and a radiologist. In this way it can be ensured that it concerns the ovarian veins.

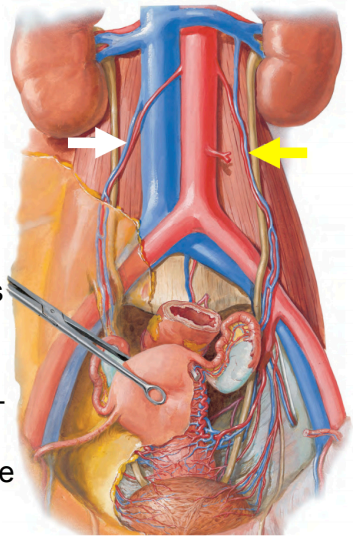

Figure 2.1: Anatomy of the abdomen. White arrow: right ovarian vein, yellow arrow: left ovarian vein [7].

2.3 Imaging sequences

The following imaging sequences are examined to determine which best image the ovarian veins. All the sequences will be performed in the axial plane, such that the diameter of the ovarian veins can be imaged. In addition, all sequences will be performed in combination with breath-hold at the $1,5$ T clinical scanner. This to reduce the respiratory artefacts as much as possible [8]. When breath-hold is not feasible in combination with the desired sequence due to the scan time, the sequence will be performed with shallow breathing or respiratory trigger. Important to realise is that breath-hold can not be used at the $0,25$ T tiltable scanner. Nevertheless, the sequences performed at the $1,5$ clinical scanner will be performed in combination with breath-hold, shallow breathing or respiratory trigger. In this way the location of the ovarian veins can be clearly imaged, which could help locate the ovarian veins in the images acquired with the $0,25$ T tiltable scanner.

2.3.1 *T_2-weighted fast spin echo sequence with breath-hold*

T_2-weighted fast spin echo sequences are important standard sequences for the assessment of pathological conditions in the female pelvis [8]. A T_2-weighted fast spin echo sequence uses a series of $180°$ refocusing pulses after a single $90°$ pulse. In this way a train of echoes is produced. With the use of this technique, the phase-encoding gradient is adjusted for each of these echoes. This allows multiple lines to be acquired in the k-space within a given repetition time (T_R). This leads to a relatively short scan time [9]. The scan time depends on the number of echoes acquired in the T_R interval, also called the echo train length (ETL). The scan time is inversely proportional to the ETL, which means that if a fast spin echo sequence has a ETL of 6, the sequence can be performed in $1/6$ of the scan time of a conventional spin echo sequence with the same T_R.
The short scan time is beneficial while imaging the abdomen and pelvis. This is because breath-hold can be implemented with a short scan time, and will lead to fewer respiratory artefacts in the images. The sequence will also be performed without breath-hold to determine what the effects of breath-hold are. In addition, a short scan time can also be beneficial when later image in upright position. In this way the volunteer would not have to be in upright position for a long scan time.

Both veins and arteries will be visible using the T_2-weighted fast spin echo sequence. The blood in the veins and arteries will appear as dark blood surrounded by the vessel walls with a high signal intensity [10]. This means that if the ovarian veins are visible with this sequence, they will appear as dark spots surrounded by vessel walls with a high signal intensity.

Besides that only the T_2-weighted fast spin echo sequence will be performed, this sequence will also be performed with fat saturation and SPAIR. These are two different ways of fat suppression in an image. With fat saturation, a short-duration frequency selective 90° RF pulse is applied. This RF pulse rotates the fat magnetization in the transverse plane. By then applying a strong spoiler gradient immediately after the 90° RF pulse, the fat magnetization will be destroyed. In this way the fat signal is suppressed [11]. The other fat suppression technique SPAIR is short for *Spectral Attenuated Inversion Recovery*. This fat suppression technique uses a 180° inverting pulse, which causes the longitudinal magnetization of fat to be in the $-$z-direction, and thus reversed. The water protons are not affected by this RF pulse. Due to the short T_1 of fat, the longitudinal magnetization of fat will quickly recover. When the longitudinal magnetization is zero, the image sequence will start. In this way, signal is only generated from the water protons and the fat signal is suppressed [12].

Images will be acquired with using only fat saturation and images will be acquired with using both fat saturation and SPAIR. These two fat suppression techniques are performed because these could lower the signal intensities of respiratory artefacts [13].

2.3.2 *T_1-weighted Dixon sequence with breath-hold*

With the help of a T_1-weighted Dixon sequence uniform fat suppression is achieved. A Dixon sequence uses the in-phase/out-of-phase cycles of water and fat. Water and fat protons have moderately different resonance frequencies. This causes their spins to go in-phase and out-of-phase with each other as a function of time. Using a Dixon sequence, the in-phase and out-of-phase images of water and fat can be combined, with the result that only water, and only fat images can be acquired [14]. A Dixon sequence will produce four sets of images: only water images, only fat images, in-phase images, and out-of-phase images. With the use of the only water images, fat suppression is obtained. These fat suppression images can be of use for the same reasons as mentioned before with the T_2-weighted fast spin echo sequence in combination with fat suppression techniques, and thus to lower the signal intensities of respiratory artefacts. The T_1-weighted Dixon sequence will also be performed in combination with breath-hold.

Similar to the T_2-weighted fast spin echo sequence, the T_1-weighted Dixon sequence will also show both veins and arteries in the images. The blood in the veins and arteries will appear as bright blood. However, the blood in the arteries will appear with higher signal intensity compared to the blood in the veins. This means that if the ovarian veins are visible with this sequence, they will appear as grey spots compared to the arteries.

2.3.3 *Time-of-flight sequence with shallow breathing*

The Time-of-flight (TOF) sequence is a non-contrast bright-blood imaging technique. The TOF sequence is based on flow-related enhancement. With this sequence, stationary tissues in an imaged volume are saturated by multiple repetitive RF pulses. These multiple RF pulses lower the steady state magnetisation levels. When 'fresh' blood flows through the imaged volume, it has not yet experienced the repetitive RF pulses. Hence, it still has a high initial magnetisation. The signal of the in flowing blood is therefore bright compared to the signal of the stationary tissues [15].

During this sequence, a saturation band will be placed at the top of the imaged volume. In this way, only 'fresh' blood flowing in from below the imaged volume will give a signal. The 'fresh' blood flowing into the imaged volume from above will be saturated by the saturation band and would not give a signal. This means that by using this saturation band, only blood flowing through the veins will give a signal. The blood flowing through the arteries will be saturated by the saturation band. The blood flowing through the veins will have a high signal intensity, which means that they appear as bright blood. This means that the ovarian veins will appear as a bright white spot on the images.

By only imaging the veins, it could become easier to recognise the ovarian veins in the images. This is because there can be no confusion between the veins and the arteries. In addition, with the use of the TOF sequence a 3D *Maximum Intensity Projection* (MIP) can be made. The 3D MIP will show a

map of the veins that are imaged with the help of the TOF sequence. In this way the course of the different veins that are imaged can be followed, and this could help confirm that the ovarian veins have been imaged.

The TOF sequence will be performed in combination with shallow breathing. The scan time of this sequence will be too long to perform the sequence in combination with breath-hold.

2.3.4 *Phase contrast MRA sequence with shallow breathing*

During a phase contrast MRA sequence, the spins are exposed to bipolar gradients. When a stationary spin is exposed to a bipolar gradient pair, it will not experience a net phase shift. However, when a moving spin is exposed to a bipolar gradient pair, it will experience a net phase shift proportional to its velocity. By measuring these phase changes, the velocity of the fluids can be determined. In this way, this MRI technique can visualise moving fluids, or in this case blood, which can be useful for imaging the ovarian veins [16].

This sequence will again be performed with the use of a saturation band placed at the top of the imaged volume. In this way only the veins will be visible on the images. The veins will appear with a high signal intensity, which means that the ovarian veins will appear with a high signal intensity. The blood in the veins will be bright blood on the images. Important to realise is that the phase contrast MRA sequence will be performed in sagittal plane. This in contrast to the other imaging sequences, which will be performed in axial plane. By performing this sequence in the sagittal plane, a map of the venous vascular structures will be produced. This could help localise the ovarian veins, by possibly imaging the course of the ovarian veins.

The degree of sensitivity to 'slow blood' or 'fast blood' can be determined by the amplitude, duration and spacing of the bipolar gradients. This can be set using the parameter Velocity Encoding (VENC). The unit of VENC is cm/s. VENC should be chosen to encompass supposable the highest velocities that can be found in the vessels of interest. For imaging the ovarian veins VENC should be equal to $10\ cm/s$ [17].

3 RESULTS

3.1 Images acquired at 1,5 T in supine position

3.1.1 *Overview of the results of imaging at 1,5 T in supine position*

Table 3.1 shows an overview of the results obtained at $1,5$ T in supine position. The table shows if the LOV and the ROV can be imaged with the help of the different performed sequences at the $1,5$ T clinical scanner in supine position. By showing an overview of the imaging sequences that can image the LOV and/or ROV, the table directly indicates which of the sequences obtain a contrast in which the ovarian veins can be imaged and therefore could be performed at the $0,25$ T tiltable scanner in upright position. The following sections will discuss the results of each imaging sequence in detail.

Results of the imaging sequences at $1,5$ T in supine position		
Sequence	**LOV**	**ROV**
T_2-weighted fast spin echo sequence	Yes	No
T_2-weighted fast spin echo sequence with fat suppression techniques	No	No
Time-of-flight sequence	No	No
T_1-weighted Dixon sequence	No	No
Phase contrast MRA sequence	No	No

Table 3.1: Overview of the results of imaging at $1,5$ T in supine position.

3.1.2 *T_2-weighted fast spin echo sequences*

T_2-weighted fast spin echo sequence with breath-hold

Figure 3.1 shows two images from the series of images acquired with the T_2-weighted fast spin echo sequence with breath-hold. The images are made from the top of L2 till the bladder.
In the left image in figure 3.1, the orange arrow points to the LRV, which is drained into the IVC. As mentioned in the method, the LRV is an important starting point for identifying the LOV in the images, because the LOV is drained into the LRV. In the right image in figure 3.1, the red arrow points to the left renal artery (LRA), which branches from the aorta.

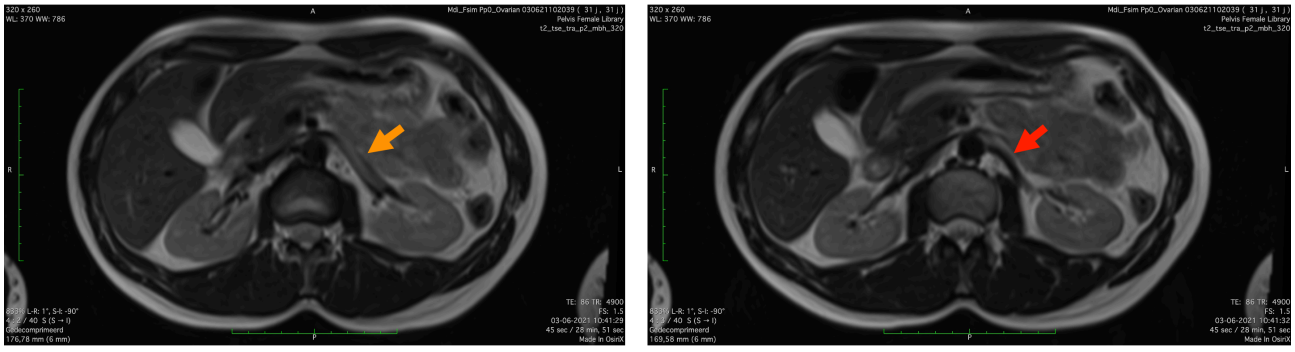

Figure 3.1: Images acquired with the T_2-weighted fast spin echo sequence with breath-hold, from the top of L2 till the bladder. Orange arrow: LRV. Red arrow: LRA.

By observing the location where the LRV was seen throughout the series of images, a structure can be seen that indicates the LOV. This is shown in the left image in figure 3.2, where the LOV is pointed to with a yellow arrow. The structure can be identified as the LOV, because in the series of images it is clearly shown how the structure indicating the LOV is drained into the LRV. In the right image in figure 3.2 the yellow arrow points to three structures together. These three structure are the LOV, the LOA, and the ureter.

The structure indicating the LOV is followed through the scans until the left ovary, the starting point of the LOV. The structure however disappears through the scans, but at the left ovary dark spots can be seen again. This is shown in figure 3.3, the dark spots are pointed to with the yellow solid arrow. The yellow dashed arrow in this figure points to the left ovary and the white dashed arrow points to the right ovary. Nevertheless, it is difficult to identify the LOV from these dark spots, because the complete course of the LOV can not be followed through the scans.

The ROV can not be identified in these series of images. A reason for this could be that the ROV coincides with the IVC, because the ROV is drained directly into the IVC.

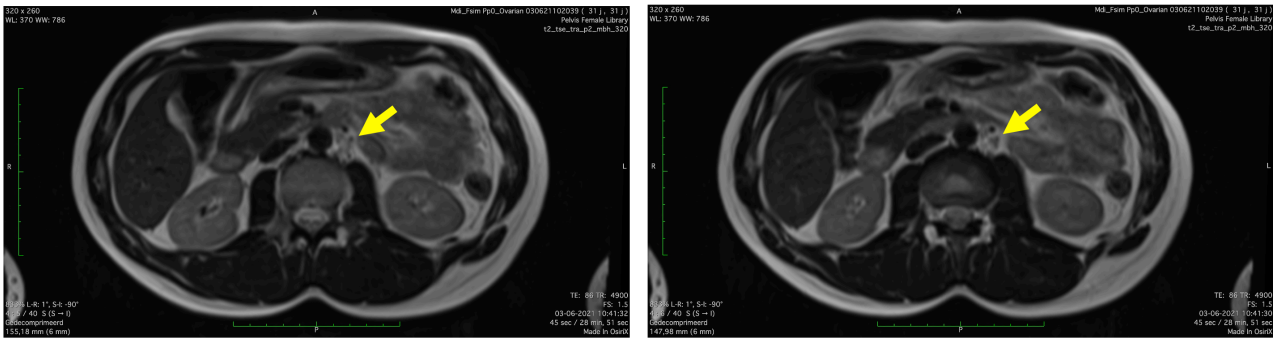

Figure 3.2: Images acquired with the T_2-weighted fast spin echo sequence with breath-hold, from the top of L2 till the bladder. The yellow arrows point in both images to the LOV.

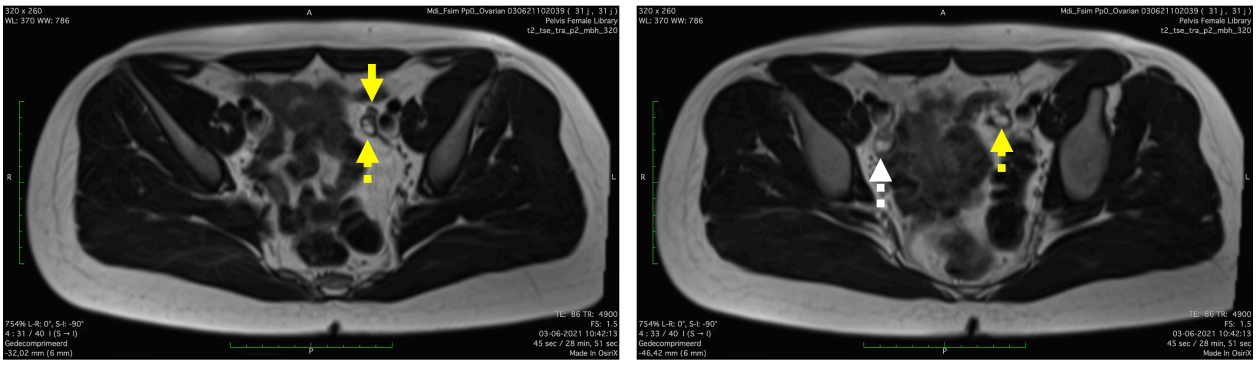

Figure 3.3: Images acquired with the T_2-weighted fast spin echo sequence with breath-hold, from the top of L2 till the bladder. The dashed arrows points to the left ovary. The yellow solid arrow points to dark spots, which one of them could be the LOV. The white dashed arrow points to the right ovary.

The sequence is also performed without breath-hold. Two images from the series of images acquired with this sequence without breath-hold are shown in figure 3.4. Respiratory artefacts are shown throughout the series of images. In the figure these respiratory artefacts are pointed to with the grey arrows. Nevertheless, the LOV can still be identified from the images. The yellow arrow in the left image points to the LOV.

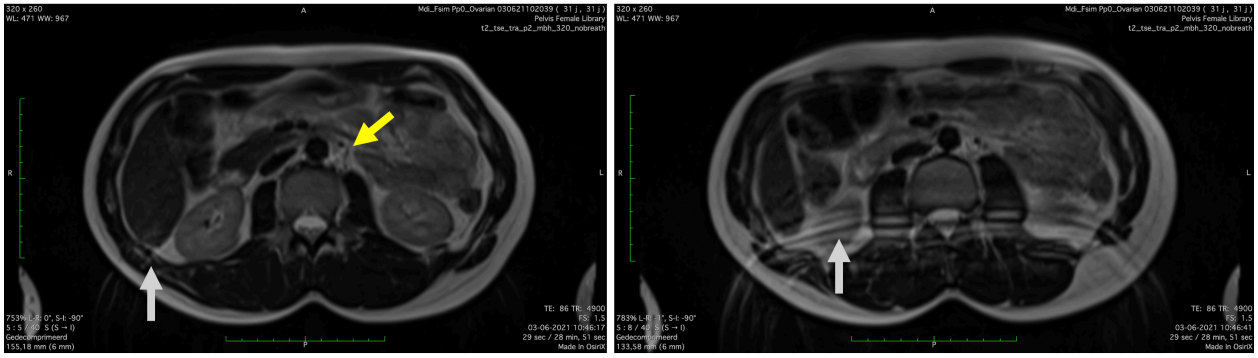

Figure 3.4: Images acquired with the T_2-weighted fast spin echo sequence without breath-hold, from the top of L2 till the bladder. The yellow arrow points to the LOV, the grey arrows point to artefacts due to respiratory movements.

T_2-weighted fast spin echo sequence with a higher resolution

The T_2-weighted fast spin echo sequence is performed again with a higher resolution. By using a higher resolution, the ROV may possibly be identified and the course of the LOV may be visible throughout the series of images. The same part of the abdomen and pelvis is imaged during this sequence, from the top of L2 till the bladder. Also, the field of view was kept the same value. The resolution was increased by increasing the image matrix from 320 x 260 to 512 x 416. The pixel spacing for the images described before was $1,1876\backslash1,875\ mm$. The pixel spacing for this sequence with the higher resolution was $0,7421875\backslash0,7421875\ mm$.

In figure 3.5 two images of the series of images acquired with a higher resolution are shown. Because of the higher resolution, the scan time was increased. Therefore the sequence could not be performed in combination with breath-hold. Instead, the sequence was performed in combination with respiratory trigger. Nevertheless, the images still show respiratory artefacts, which reduce the image quality. The grey arrows in both images point to examples of these artefacts. Despite the respiratory artefacts, a structure is shown that may indicate the LOV. However, due to the artefacts, it is difficult to reliably identify this structure as the LOV. The yellow arrow in both images points to the structures that may indicate the LOV. Also, due to the respiratory artefacts, the course of the structure that may indicate the LOV could again not be followed and the ROV can again not be identified in these images.

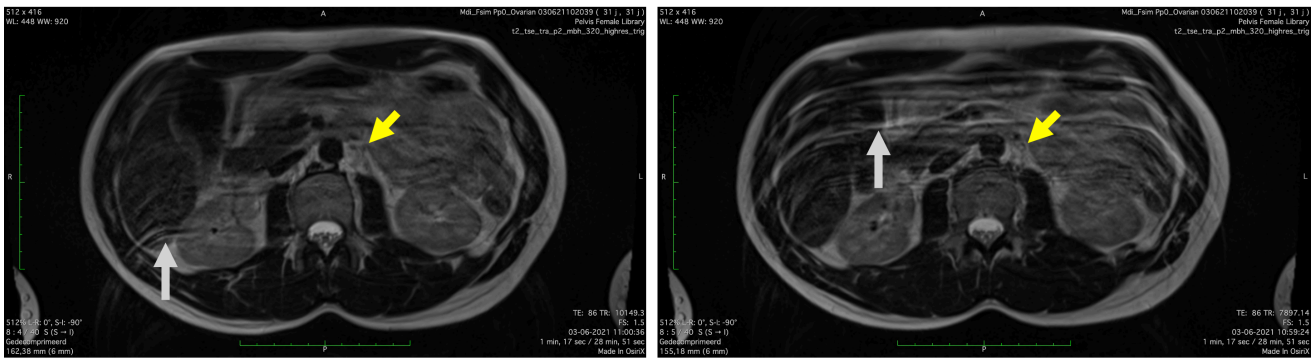

Figure 3.5: Images acquired with the T_2-weighted fast spin echo sequence with a higher resolution and respiratory trigger, from the top of L2 till the bladder. The yellow arrows in both images point to a structure that may indicate the LOV, the grey arrows point to artefacts due to respiratory movement.

T_2-weighted fast spin echo sequence performed in other healthy female volunteers

The T_2-weighted fast spin echo sequence is performed once more in two different healthy female volunteers. This to determine whether the LOV can also be imaged with the T_2-weighted fast spin echo sequence in different women. In figure 3.6 two images are shown from a series of images that are made of two different healthy female volunteers. In the left image the yellow arrow points to three structures that can be identified as the LOV, the LOA and the ureter. However, this is difficult to determine with certainty because this sequence is performed in a relatively small part of the abdomen, which means that these structures could not be followed until the ovaries. In addition, the LRV is also not visible in these series of images, which also contributes in identifying the LOV. In the right image a structure is also shown which may indicate the LOV. The structure is pointed to with the yellow arrow. Again, it is difficult to determine with certainty if this structure is the LOV. The structure is followed until the left ovary, but the structure disappear through the images and the LRV is again not visible in these series of images. The ROV is not visible in both of the series of images.

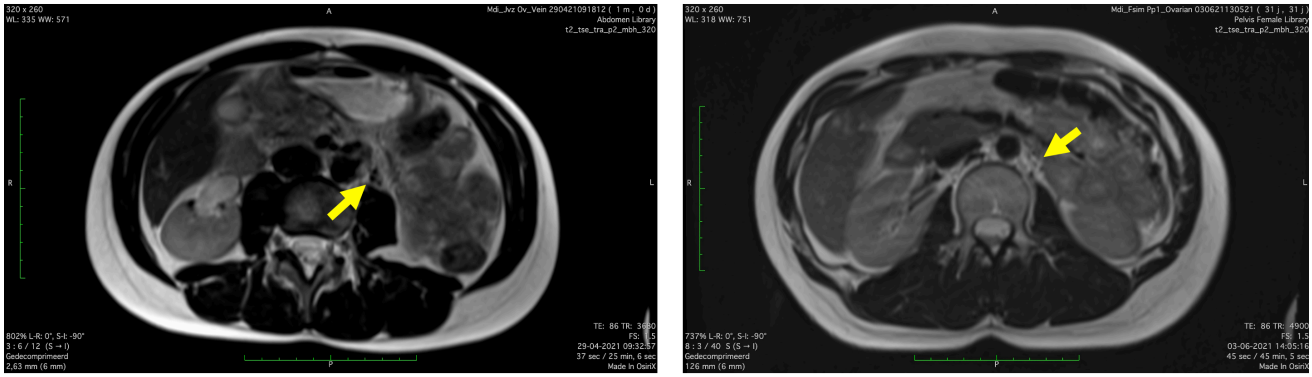

Figure 3.6: Images acquired by the T_2-weighted fast spin echo sequence with breath-hold; the left and right image are acquired from two different healthy female volunteers. The yellow arrow in both images point to possible LOV structures.

T_2-weighted fast spin echo sequence with fat saturation and SPAIR

Two images of the series of images acquired with T_2-weighted fast spin echo sequence with fat saturation and SPAIR are shown in figure A.1 in Appendix A.1.1. In both the images acquired with only fat suppression and the images acquired with fat suppression and SPAIR the LOV and ROV can not be identified. The contrast obtained with this sequence is not correct for imaging the ovarian veins.

3.1.3 *Time-of-flight sequences*

Time-of-flight sequence with shallow breathing

Figure 3.7 shows two images of the series of images acquired with the time-of-flight (TOF) sequence. The images are made from halfway L2 till L5.
The orange arrow in the left image in figure 3.7 points to the LRV. The LRV is again an important starting point for identifying the LOV in the images. By observing the location of LRV throughout the series of images, a structure is shown close to the LRV, which is pointed to with the blue arrow in the right image in figure 3.7. This structure may indicate the LOV, when drained into the LRV. However, this structure could also indicate the inferior mesentric vein, because the inferior mesentric vein is located approximately at the same level. The orange arrow in the right image again points to the LRV.

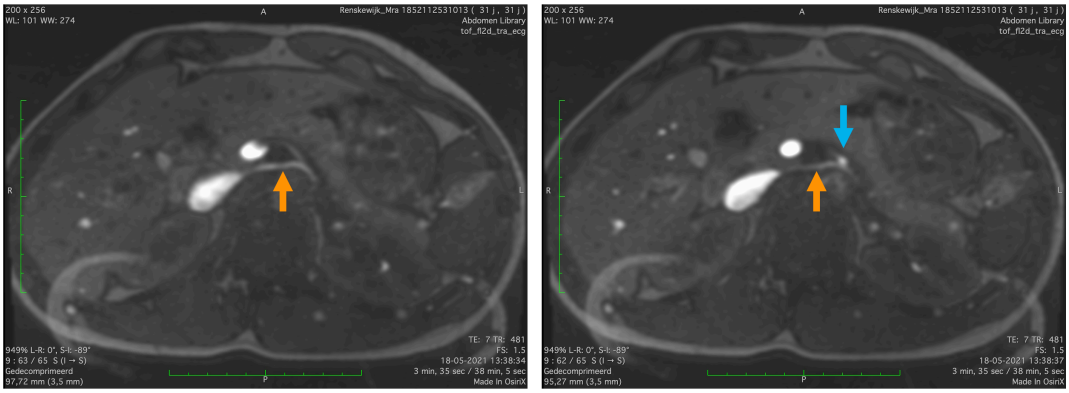

Figure 3.7: Images acquired with the time-of-flight sequence with shallow breathing, from halfway L2 till L5. The orange arrows point the LRV, the blue arrow points to inferior mesentric vein.

If the course of the structure that may indicate the LOV or the inferior mesenteric vein is followed through the series of images, the structure later splits into two veins. These two veins move further and further apart from each other throughout the series of images. The LOV also splits off later in the abdomen into two veins, but they stay together through the abdomen, which means that this structure, pointed to with the blue arrow, could not be the LOV, and therefore is the inferior mesentric vein. The ROV can not be identified in these series of images.

The images of figure 3.7 are acquired of a relatively small part of the abdomen. To confirm with certainty that the structure, pointed at with the blue arrow, is the inferior mesentric vein, the TOF sequence is performed again over a larger part of the abdomen and pelvis. In this way the course of the structure can be followed. In addition, by imaging a larger part of the abdomen and pelvis, a larger 3D MIP can be made. In figure 3.8 and 3.9 four images are shown of these series of images, which were acquired from the the top of L1 till the bottom of the spine.

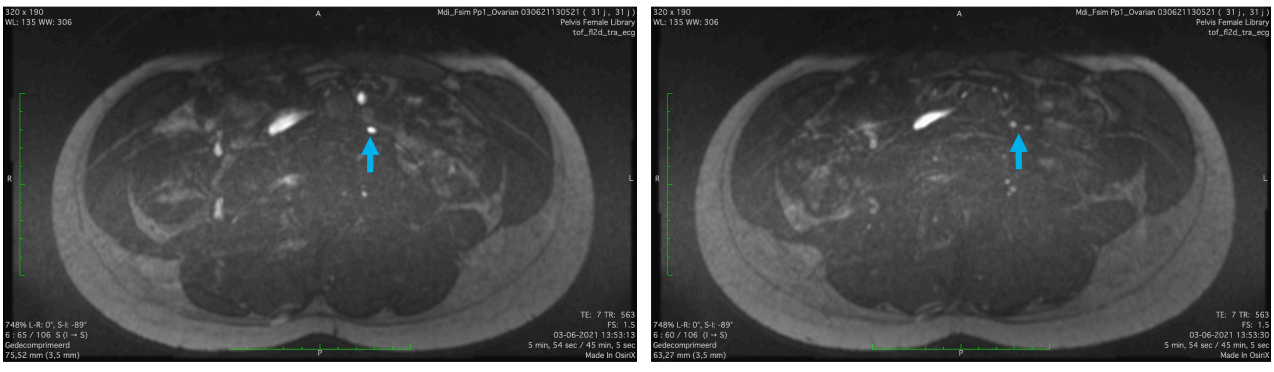

Figure 3.8: Imaged acquired with the time-of-flight sequence with shallow breathing, from the top of L1 till the bottom of the spine. The blue arrows point to inferior mesentric vein, which splits into two in the right image.

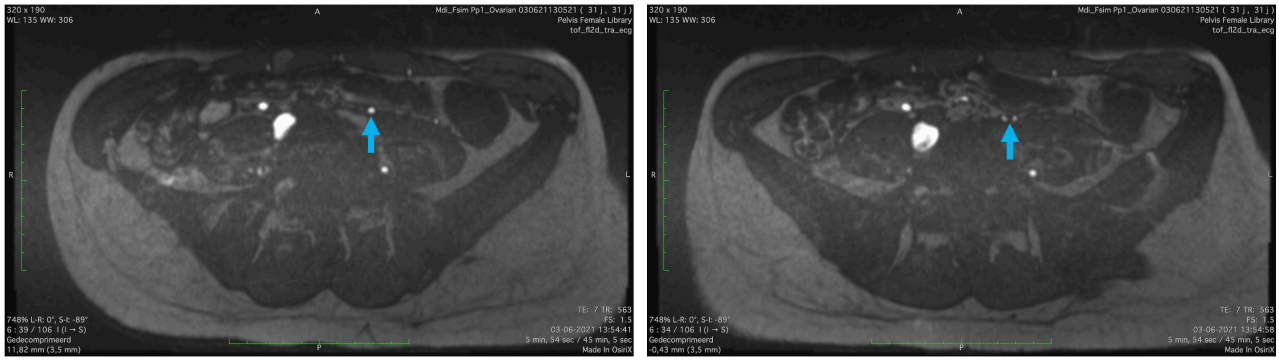

Figure 3.9: Imaged acquired with the time-of-flight sequence with shallow breathing, from the top of L1 till the bottom of the spine. The blue arrow points again at the split off.

The blue arrow in all four images in figure 3.8 and 3.9 point to the same structure, which indicates the inferior mesentric vein. In the right image in figure 3.8 the structure splits for the first time into two veins. This is the same split as mentioned before at figure 3.7. In the images in figure 3.9 the vein splits again into two veins. These veins that splits off move again further and further apart through the series of images. For this reason, it can be said with certainty that this structure is not the LOV, and is the inferior mesentric vein. The ROV is again not visible in these series of images.

3D Maximum Intensity Projection

With the help of the Time-of-flight (TOF) sequence a 3D MIP can be made. The 3D MIP image for the performed TOF sequence is shown in figure 3.10. The 3D MIP image is made with the TOF sequence, which is made from the top of L1 till the bottom of the spine. The green arrow in the image points to the structure of the IVC, which is split into the common iliac veins at the bottom of the image. The blue arrow in the image points to a structure that could be the inferior mesentric vein. But this is difficult to say with certainty. Both LOV and ROV are not visible in the image.

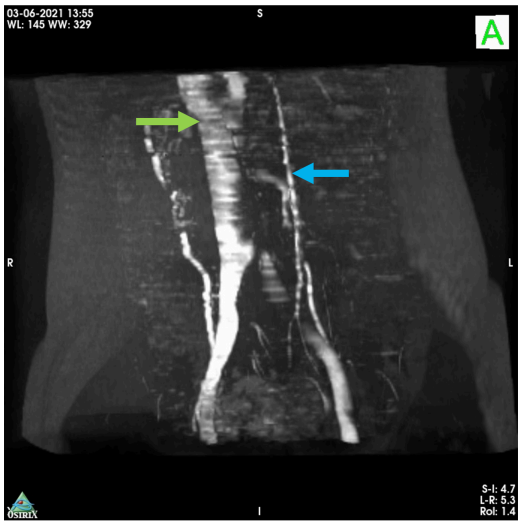

Figure 3.10: The 3D MIP from the top of L1 till the bottom of the spine. The green arrow points to the IVC, the blue arrow points to a structure that could be the inferior mesentric vein.

3.1.4 *T_1-weighted Dixon sequence with breath-hold*

In figure A.2 in Appendix A.1.2 two images are shown from the series of only water images acquired with the T_1-weighted Dixon sequence with breath-hold. In these images mainly arteries are shown, which have a high signal intensity. The veins are difficult to distinguish in contrast obtained in these images, which makes it difficult to identify the ovarian veins.

3.1.5 *Phase contrast MRA sequence with shallow breathing*

With the use of the phase contrast MRA sequence the ovarian veins can not be identified. The images have a low image quality, which makes it not only difficult to identify the LOV or ROV, but also to identify other anatomical structures. For examples of the images see figure A.3 in Appendix A.1.3.

3.2 Images acquired at 0,25 T in upright position

As shown and described in the results obtained with the $1,5$ T clinical scanner in supine position, the T_2-weighted fast spin echo sequence can image the LOV. The contrast obtained with this sequence allowed the LOV to be identified from the images. The other performed sequences obtained a contrast in which the LOV and ROV could not be identified. For these reasons, the T_2-weighted fast spin echo sequence is performed again with the $0,25$ T tiltable scanner in upright position. The parameters used for the T_2-weighted fast spin echo sequence in upright position are shown in table A.1 in Appendix A.2.1.

3.2.1 *T_2-weighted fast spin echo sequences*

T_2-weighted fast spin echo sequence

Figure 3.11 shows two images from the series of images acquired with the T_2-weighted fast spin echo sequence in upright position. In the left image the pink dashed arrow and the pink solid arrow point respectively to the right kidney and the left kidney. In this image the green solid arrow points to the IVC and the green dashed arrow points to the aorta. The orange arrow points to a structure that may indicate the LRV, as it is drained into the IVC. This is however difficult to determine which certainty, because the images have many artefacts due to intestinal peristalsis close to the location of the LRV. In the right image the orange arrow points again to the structure that may indicate the LRV. The red arrow points in this image to the LRA, as it branches from the aorta.

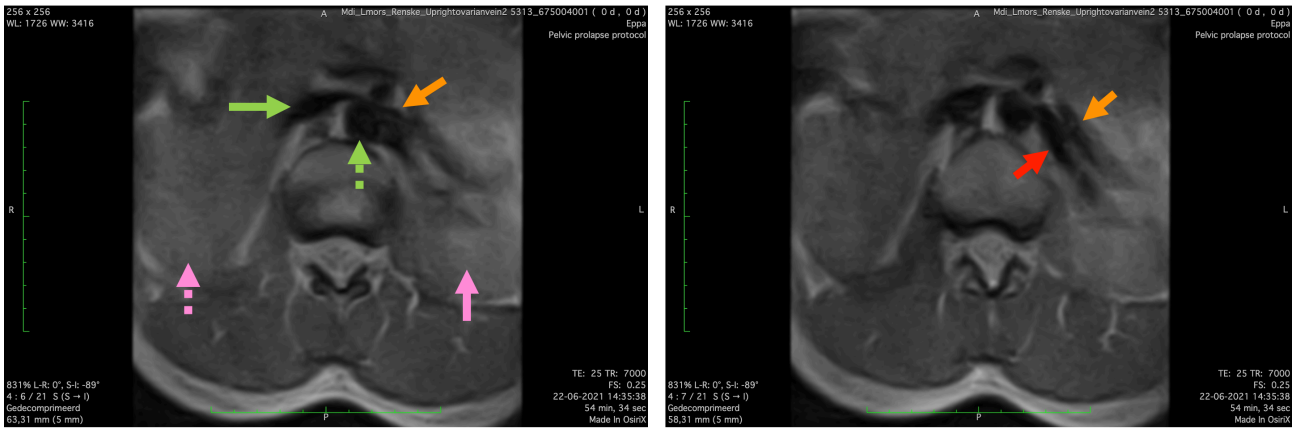

Figure 3.11: Images acquired with the T_2-weighted fast spin echo sequence in upright position. Pink dashed arrow: right kidney, pink solid arrow: the left kidney. Green solid arrow: inferior vena cava, green dashed arrow: aorta. Orange arrow in both images: left renal vein. Red arrow: LRA.

By observing the location where possibly the LRV was shown in figure 3.11, structures are seen which may indicate the LOV. These structures are shown in figure 3.12, which are pointed to with the yellow arrows. In the right image two structures are shown. Both of these structures could indicate the LOV.

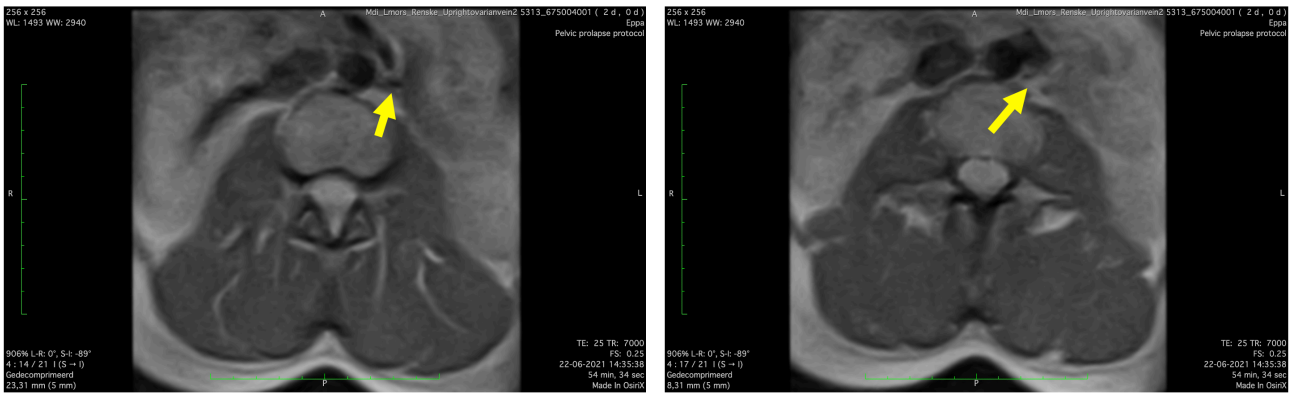

Figure 3.12: Images acquired with the T_2-weighted fast spin echo sequence in upright position. Yellow arrows point to structures that may indicate the LOV.

The structures in both of the images that may indicate the LOV disappear quickly throughout the series of images. In this way the course of the structures could not be followed, which makes it difficult to reliably identify these structures. In addition, other anatomical structures which can contribute to identifying the LOV, can not be identified either in these images, possibly as a result of artefacts due to intestinal peristalsis. For these reasons, it makes it difficult to identify these structures, pointed to with the yellow arrows, and thus makes it difficult to reliably identify the LOV. The ROV is again not visible in these images.

T_2-weighted fast spin echo sequence with a higher resolution

The T_2-weighted fast spin echo sequence was performed again with a higher resolution in upright position. By performing this sequence again with a higher resolution, new structures may become visible which can indicate the LOV and ROV, and the surrounding structures may be identified. During this sequence the same part of the abdomen and pelvis was imaged. Also, the field of view was kept the same value. The resolution was increased by increasing the image matrix from 256 x 256 to 512 x 512. The pixel spacing for the images acquired with the $0,25$ T tiltable scanner as described before was $1,09375\backslash1,09375\ mm$. The pixel spacing for this sequence with the higher resolution was $0,546875\backslash0,546875\ mm$. The number of averages in the images with a higher resolution was 1. Because it was too difficult for the volunteer to be in upright position again during this sequence, the sequence is performed in supine position.

Figure 3.13 shows two images of the series of images acquired with a higher resolution. In the left image the orange dashed arrow points to the right renal vein (RRV) and the orange solid arrow points to a structure that may indicate the LRV. The red arrow points to the LRA. By again observing the location where the LRV was shown in the images, a structure shows which may indicate the LOV. This structure is pointed to with the yellow arrow in the right image.

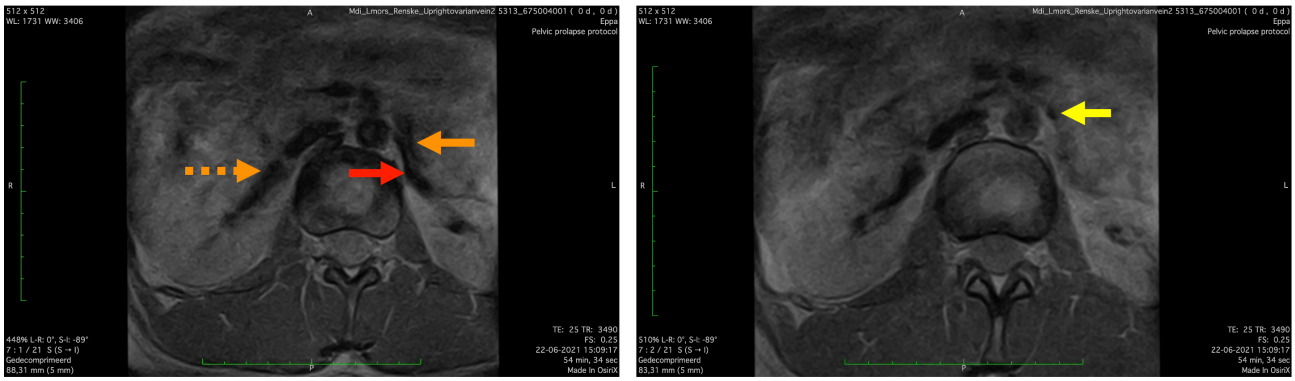

Figure 3.13: Images acquired with the T_2-weighted fast spin echo sequence with a higher resolution in supine position. Yellow arrow points to a structure that may indicate the LOV.

Again, it is difficult to determine with certainty if this structure concerns the LOV. This is because the artefacts due to intestinal peristalsis make the anatomical recognition of possibly the LOV and the surrounding structures difficult.

3.2.2 *Supine position vs. upright position*

In figure 3.14 two images are shown, both acquired with the T_2-weighted fast spin echo sequence. The left image is acquired in supine position, and the right image is acquired in upright position. Both of the images are the same slice. In the two images is a clear increase in cross-sectional area shown of the IVC when imaging in upright position. The mean cross-sectional area for the IVC in both supine and upright position is calculated over all the images, this is shown in table 3.2. The cross-sectional area of the IVC is increased with approximately 160%. This increase in cross-sectional area of the IVC in upright position indicates that imaging in upright position certainly causes dilation in the veins, which makes them more clearly visible in the images.

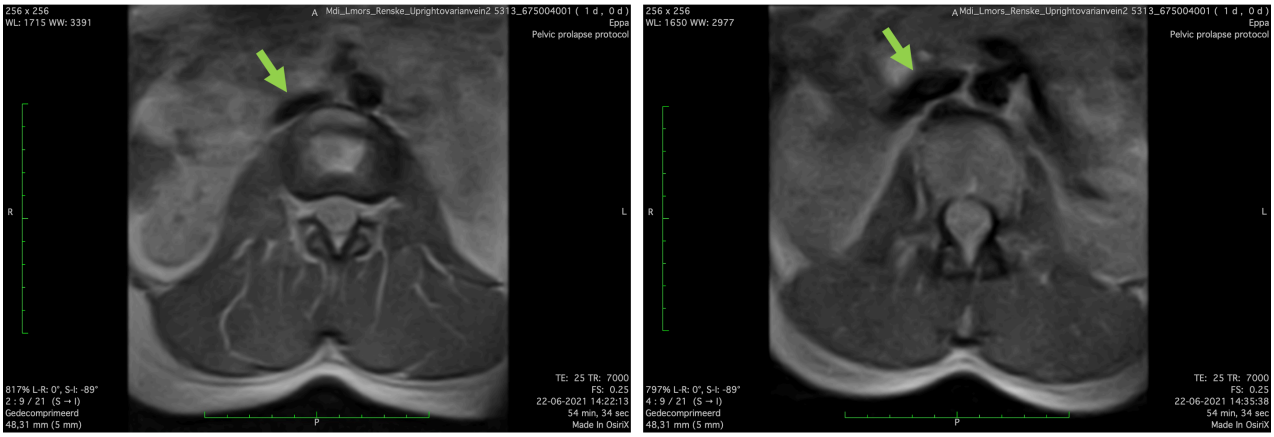

Figure 3.14: Images acquired with the T_2-weighted fast spin echo sequence. The left image is acquired in supine position, and the right image is acquired in upright position. The green arrow points to the IVC.

Position	Mean cross-sectional area of IVC	Standard deviation
Upright position	$2,9590\ cm^2$	$1,0760$
Supine position	$1,1373\ cm^2$	$0,3002$

Table 3.2: Mean cross-sectional area of the inferior vena cava in upright and supine position.

4 CONCLUSION

The goal of this thesis was to image the ovarian veins in healthy female volunteers with the help of a $0,25$ T tiltable scanner in upright position, and with that to develop an optimal imaging protocol for imaging the ovarian veins in upright position.

From the results obtained during this study, it can be concluded that the optimal imaging protocol for imaging the ovarian veins with the $0,25$ T tiltable scanner in upright position should include the T_2-weighted fast spin echo sequence performed in the axial plane. By using this sequence, a contrast can be obtained in the images which allows the LOV to be identified. This as seen in the images acquired with this sequence at a field strength of $1,5$ T in supine position. At the field strength of $0,25$ T in upright position, structures were also imaged which may indicate the LOV by using the T_2-weighted fast spin echo sequence. However, due to the inability to recognise other surrounding structures as a result of the artefacts due to intestinal peristalsis, and the need to follow the course of possibly the LOV, it could not be said with certainty whether these structures concern the LOV. Nevertheless, the contrast obtained with the T_2-weighted fast spin echo sequence at both a field strength of $1,5$ T and $0,25$ T can be correct for imaging the ovarian veins in upright position. Further research needs to be done to optimise this imaging protocol, to enable to image both the LOV and ROV with certainty in upright position by using the $0,25$ T tiltable scanner.

This study had the goal to develop an imaging protocol for imaging the ovarian veins in upright position, because this could contribute in the research for diagnosing PVCS. Nevertheless, as mentioned before, the imaging of both the ovarian veins in upright position has not yet been successful. However, as shown in the acquired images, veins do show dilation while imaging in upright position. As can be seen in the obtained results, the cross-sectional area of the IVC is increased by 160% by imaging in upright position. This could mean that the pelvic varices, due to PVCS, can also increase in cross-sectional area when imaging in upright position, and may become clearly visible in the images. This means that using the $0,25$ T tiltable scanner in upright position can still possibly contribute in diagnosing PVCS. Further research can possibly prove this.

5 DISCUSSION

During this research, it became apparent that imaging the ovarian veins in healthy women using the $0,25$ T tiltable scanner in upright position is a challenge. The anatomical recognition of the ovarian veins is difficult in the acquired images. Consequently, in the results is shown that structures are imaged which may indicate the LOV by using the T_2-weighted fast spin echo sequence but cannot be reliably identified from the acquired images. The causes underlying this difficult recognition of the ovarian veins needs to be addressed in further research in order to optimise the imaging protocol, resulting from this study.

An important cause of the difficult anatomical recognition of the ovarian veins are the artefacts due to intestinal peristalsis. In the images acquired with the $0,25$ T tiltable scanner in upright position obvious artefacts are seen at the top of the images due to intestinal peristalsis. These artefacts create blurry effects over the images, making the anatomical structures in and around these artefacts difficult to recognise. Because the female volunteers were slim, the area where the ovarian veins could be visible is close to the source of the artefacts. This makes anatomical recognition of structures that may indicate the ovarian veins difficult. In addition, this also makes the anatomical recognition of structures around possibly the ovarian veins difficult, while the recognition of these structures contributes to the confirmation that it concerns the ovarian veins.
There are several possibilities to reduce the artefacts resulting from intestinal peristalsis. First, the volunteer can fast for four hours prior to the MRI examination. However, this can be dangerous for the volunteer while imaging in upright position. Another possibility to reduce the artefacts could be the administration of antispasmodic agents. These agents effectively reduce intestinal peristalsis. An example of an antispasmodic agent is *Hyoscine Butylbromide*. This can be administrated five to ten minutes prior to the MRI examination [13]. Further research will have to be done on the potential risks of the use of antispasmodic agents for the volunteer or patient, when imaging in upright position.

Using a higher resolution while imaging in upright position may also improve the anatomical recognition of the ovarian veins, and thus contribute to optimising the imaging protocol. During this study, images with a higher resolution have already been acquired in supine position at $0,25$ T, this as can be seen in the results. In the images acquired with a higher resolution, the anatomical structures are more clearly visible. An even higher resolution could therefore potentially lead to better anatomical recognition of the ovarian veins. In addition, a higher resolution could help image structures that may indicate the ROV. This has not yet been achieved in any scan acquired in this study.
However, increasing the resolution brings disadvantages. Increasing the resolution leads to a decrease in signal to noise ratio (SNR). A decrease in SNR can lead to grainy images. Another disadvantage as a result of increasing the resolution, is an increase in the scan time, which is not beneficial when imaging in upright position. A solution for this could be to reduce the field of view to only the area of interest. In the images acquired during this study, a large part of the back muscles and part of the liver are also imaged. While these structures do not contribute to the anatomical recognition of the ovarian veins as shown in the scans acquired at $1,5$ T, in which the LOV is imaged. However, decreasing the field of view, by for example decreasing the number of phase encoding steps, may cause a wrap around (aliasing) artefact which can again inhibit the anatomical recognition of the ovarian veins [18]. Also, this may again cause a decrease in SNR. Further research will have to be done to determine how these different parameters can be adjusted to each other.

Important to realise when deciding to image with a higher resolution, is that when looking at the images acquired in this study with a lower resolution in upright position, the blood circulation in the back muscles is clearly visible. This means that the resolution achieved in these images may also be

able to image the ovarian veins. Nevertheless, this only applies when the appropriate measures are taken against the artefacts due to the intestinal peristalsis.

Finally, imaging a larger part of the abdomen and pelvis in upright position during future research, may also contribute to the anatomical recognition of the ovarian veins. By imaging a larger part of the abdomen and pelvis, the course of the structures that may indicate the ovarian veins can be followed. By following the course of these structures, it can be determined with certainty whether these structures concern the ovarian veins. The images, as made in this study, are acquired in terms of the spine from the top of L2 till halfway L4. One possibility could be to image from the top of L2 till the ovaries, because the ovaries are, as mentioned before, the starting point of the ovarian veins. A disadvantage of increasing the part of the abdomen and pelvis that is imaged, is that the scan time will also increase. Which could mean that the volunteer may have to stand twice the scan time in upright position. A solution for this could be to divide the scans, and not immediately make the full scan from the larger part of the abdomen and pelvis. In this way the volunteer can move her feet and hands in between the scans.
However, it is not certain whether the course of the ovarian veins can be imaged using the $0,25$ T tiltable scanner in upright position. The course of the structure that indicated the LOV in the images acquired at $1,5$ T could not be followed either, the LOV was not visible in the images lower in the abdomen. This is important to take into account during future research.

When examining possible adjustments to optimise the imaging protocol during future research, the volunteer or patient being scanned in upright position should always be considered. Scanning in an upright position can be strenuous and hard for the patient or volunteer. While acquiring the images in upright position during this study, a volunteer almost fainted. The volunteer indicated after approximately ten minutes of standing in upright position that she suddenly felt light-headed. This can be caused by standing in upright position for a long time without movement. The blood pressure can drop quickly, which can lead to fainting. This can also arise if the patient is frequently moved from supine to upright position and vice versa. It is therefore important when using the $0,25$ T tiltable scanner to keep checking on the patient or volunteer, and when optimising the imaging protocol during future research the volunteer or patient is always considered.

Fewer studies have been done on imaging the ovarian veins using MRI in healthy women. A reason for this could be that when the ovarian veins are not affected by PVCS, they have a much smaller diameter, which makes it difficult to reliably identify them in the acquired images. A cadavar study has shown that the LOV has a mean diameter of $4,20 \pm 0,96\ mm$, and the ROV has a mean diameter of $3,66 \pm 1,18\ mm$, whereas the diameter of the ROV is often smaller than the diameter of the LOV [19]. This in contrast to ovarian veins affected by PVCS, where the diameter varies between 5 to 10 mm [3]. The increased diameter due to the PVCS makes it easier to image the ovarian veins, simply because they are more conspicuous in the images [10]. Therefore, it should be taken into account that there is a possibility that despite the dilation due to scanning in upright position, the diameter of the ovarian veins in healthy women is still too small to image, and that both the ovarian veins can only be imaged in pathological condition using MRI.

REFERENCES

[1] Jane P. Daniels and Khalid S. Khan. Chronic pelvic pain in women. *BMJ (Online)*, 341(7776):772–775, oct 2010.

[2] M. H. Meissner and K. Gibson. Clinical outcome after treatment of pelvic congestion syndrome: Sense and nonsense. *Phlebology*, 30(1 Suppl):73–80, mar 2015.

[3] Chiara Borghi and Lucio Dell'Atti. Pelvic congestion syndrome: the current state of the literature. *Archives of Gynecology and Obstetrics*, 293(2):291–301, 2016.

[4] V. Juhan. Chronic pelvic pain: An imaging approach. *Diagnostic and Interventional Imaging*, 96(10):997–1007, oct 2015.

[5] Vivak Hansrani, Zainab Dhorat, and Charles N. McCollum. Diagnosing of pelvic vein incompetence using minimally invasive ultrasound techniques. *Vascular*, 25(3):253–259, 2017.

[6] Mitsue Miyazaki and Hiroyoshi Isoda. Non-contrast-enhanced MR angiography of the abdomen. *European Journal of Radiology*, 80(1):9–23, oct 2011.

[7] F H Netter. *Atlas of Human Anatomy*. Elsevier Inc., 6 edition, 2011.

[8] Takayuki Masui, Motoyuki Katayama, Shigeru Kobayashi, Harumi Sakahara, Tatsuhiko Ito, and Atsushi Nozaki. T2-weighted MRI of the female pelvis: Comparison of breath-hold fast-recovery fast spin-echo and nonbreath-hold fast spin-echo sequences. *Journal of Magnetic Resonance Imaging*, 13(6):930–937, jun 2001.

[9] Borut Weishaupt, Dominik, Köchli, Victor D., Marincek. Fast Pulse Sequences. In *How Does MRI Work?*, chapter 8, pages 57–62. Springer Berlin Heidelberg, 2nd edition, jan 2008.

[10] L M Leiber, F Thouveny, A Bouvier, M Labriffe, E Berthier, C Aubé, and S Willoteaux. MRI and venographic aspects of pelvic venous insufficiency. *Diagnostic and Interventional Imaging*, 95(11):1091–1102, 2014.

[11] E. De Kerviler, A. Leroy-Willig, O. Clément, and J. Frija. Fat suppression techniques in MRI: An update. *Biomedicine and Pharmacotherapy*, 52(2):69–75, 1998.

[12] T Lauenstein. Spectral Adiabatic Inversion Recovery (SPAIR) MR imaging of the Abdomen, 2008.

[13] Khashayar Rafat Zand, Caroline Reinhold, Masoom A. Haider, Asako Nakai, Laurian Rohoman, and Sharad Maheshwari. Artifacts and pitfalls in MR imaging of the pelvis. *Journal of Magnetic Resonance Imaging*, 26(3):480–497, sep 2007.

[14] Jingfei Ma. Dixon Techniques for Water and Fat Imaging. *JOURNAL OF MAGNETIC RESONANCE IMAGING*, 28:543–558, 2008.

[15] D. Saloner. The AAPM/RSNA physics tutorial for residents. An introduction to MR angiography. *Radiographics : a review publication of the Radiological Society of North America, Inc*, 15(2):453–465, 1995.

[16] David T. Wymer, Kunal P. Patel, William F. Burke, and Vinay K. Bhatia. Phase-contrast MRI: Physics, techniques, and clinical applications. *Radiographics*, 40(1):122–140, 2020.

[17] L. Q. Meneses, S. Uribe, C. Tejos, M. E. Andía, M. Fava, and P. Irarrazaval. Using magnetic resonance phase-contrast velocity mapping for diagnosing pelvic congestion syndrome. *Phlebology*, 26(4):157–161, jun 2011.

[18] Elizabeth Pusey, Chun Yoon, Michael L. Anselmo, and Robert B. Lufkin. Aliasing artifacts in mr imaging. *Computerized Medical Imaging and Graphics*, 12(4):219–224, 1988.

[19] Anasuya Ghosh and Subhramoy Chaudhury. A cadaveric study of ovarian veins: Variations, measurements and clinical significance. *Anatomy and Cell Biology*, 52(4):385–389, 2019.

A APPENDIX

A.1 Imaging at 1,5 T in supine position

A.1.1 *T_2-weighted fast spin echo sequence with fat saturation and SPAIR and breath-hold*

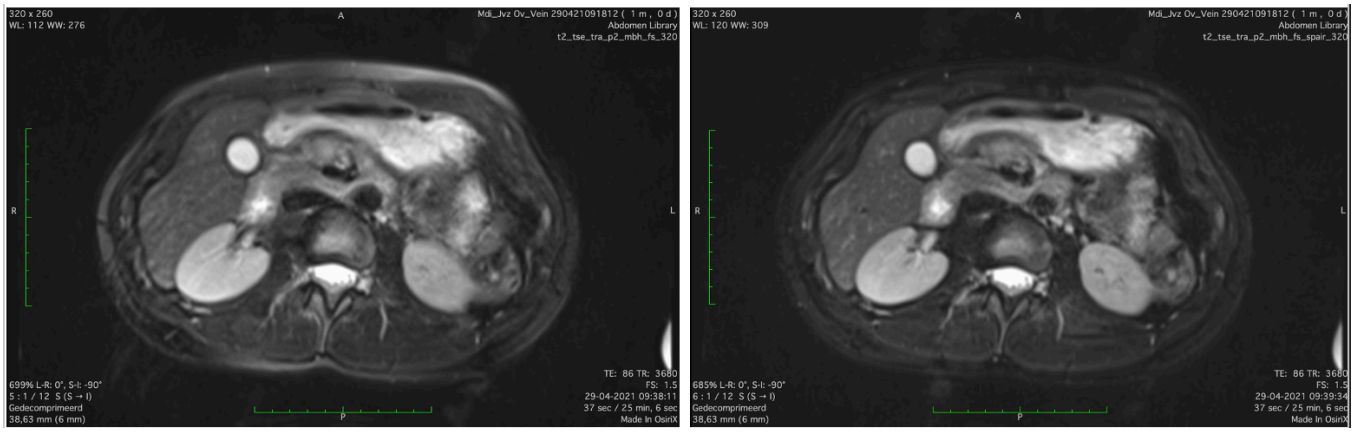

Figure A.1: Left image: acquired by the T_2-weighted fast spin echo sequence with fat saturation. Right image: acquired by the T_2-weighted fast spin echo sequence with fat saturation and SPAIR.

A.1.2 *T_1-weighted Dixon sequence with breath-hold*

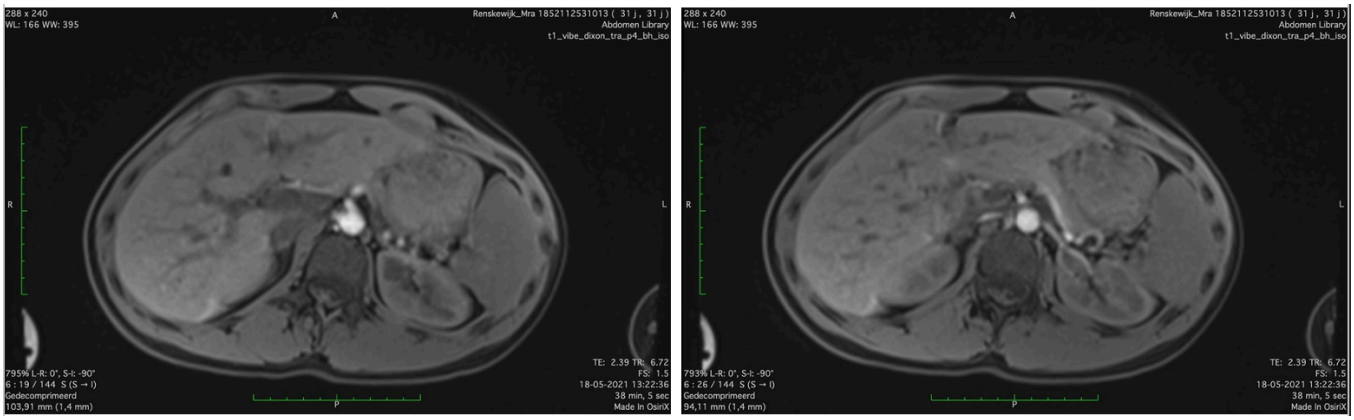

Figure A.2: Images acquired by the T_1-weighted Dixon sequence with breath-hold; water-only images, from halfway L2 till L5.

A.1.3 *Phase contrast MRA sequence*

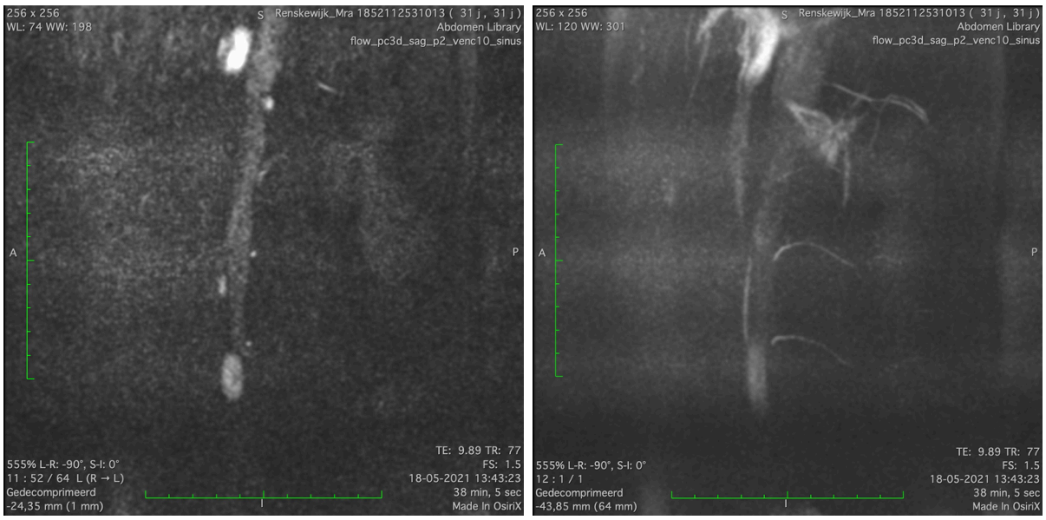

Figure A.3: Images acquired by the Phase contrast MRA sequence with shallow breathing with VENC = $10\ cm/s$*, from halfway L2 till L5.*

A.2 Imaging at 0,25 T in upright position

A.2.1 *Settings of the parameters of the T_2-weighted fast spin echo sequence in upright position*

The parameters of T_2-weighted fast spin echo sequence in upright position	
Protocol name	Pelvic Prolapse Protocol
Repetition time	7000
Echo time	$25\ ms$
Encoding field of view	$280\ mm$
Readout field of view	$280\ mm$
Number of averages	2
Rows	256
Columns	256
Flip angle	$90°$
Slice thickness	$5\ mm$
Echo train length	10

Table A.1: Settings of the parameters for the T_2-weighted fast spin echo sequence in upright position at the $0,25$ *T tiltable scanner.*